Supplement of Atmos. Meas. Tech., 18, 4631–4645, 2025
https://doi.org/10.5194/amt-18-4631-2025-supplement

Atmospheric Measurement Techniques
Open Access

Supplement of

Best practices and uncertainties in CH_4 emission quantification: employing mobile measurements and Gaussian plume modelling at a biogas plant

Julia Beate Wietzel et al.

Correspondence to: Julia Beate Wietzel (jwietzel@iup.uni-heidelberg.de)

Figure S1. Satellite view on parking lot Mannheim. Controlled release experiments were carried out between November 2018 and October 2020 (© Google Earth 2025).

Figure S2. Satellite view on airfield Heidelberg. Controlled release experiments were carried out in October 2023 (© Google Earth 2025).

Instrument	Measured Species	Temporal resolution [Hz]	Precision	Date of Use
LI-7810 (Licor)	CH_4, CO_2, H_2O	1	0.4 ppb (1 s, 2 ppm CH_4), 1 ppb (1 s, 10 ppm CH_4)	Since 10/2019
G2201-i (Picarro)	CH_4, CO_2, H_2O, $\delta^{13}CH_4$, $\delta^{13}CO_2$	0.27	0.3 ppb (3.7 s, 2 ppm CH_4), 2.7 ppb (3.7 s, 10 ppm CH_4)	Until 09/2019
Vantage Pro2 (Davis Instruments)	WS,WD,T,h p	0.16	1 m/s (5%, WS)	Until 05/2018
Ultrasonic 3D-anemometer USA-1 (Metek)	WS,WD,T,u,v,w	1	± 0.01 m/s (WS)	Since 01/2019
MaxiMet GMX500 2D-anemometer (Gill)	WS,WD,T, h,p	1	3%, WS	Since 05/2018
GPS logger (Navilock)	Lat, Long, Altitude	1	3 m	Until end 2020
GPS logger (BasicAirData)	Lat, Long, Altitude, Speed	1	3 m	Since beginning 2020

Table S1. Analyzers, measured species and specification of measurement instruments.

WS [m s^{-1}]	Incoming solar Radiation		
	Strong	Moderate	Slight
< 2	A	A - B	B
2 – 3	A - B	B	C
3 – 5	B	B - C	C
5 – 6	C	C - D	D
6 <	C	D	D

Table S2. Atmospheric stability classes by Pasquill for daytime incoming solar radiation (Hanna et al., (1982), Turner (1970)).

Stability class	σ_y	σ_z
A	$0.22x(1+0.0001x)^{-1/2}$	0.20x
B	$0.16x(1+0.0001x)^{-1/2}$	0.12x
C	$0.11x(1+0.0001x)^{-1/2}$	$0.08x(1+0.0002x)^{-1/2}$
D	$0.08x(1+0.0001x)^{-1/2}$	$0.06x(1+0.00015x)^{-1/2}$

Table S3. Briggs parametrisation for stability classes (x is distance), Hanna et al., (1982).

(a)

(b)

Figure S3. Measurement setup for mobile measurements with (a) showing the roof system with air inlet and mobile anemometer and (b) stationary anemometer installed on a tripod.

Instrument	Integral meas [kg m^{-2}]	Integral mod [kg m^{-2}]	Estimated Q [kgCH$_4$ h^{-1}]
OF-CEAS	0.00012	0.00012	2.63
CRDS	0.00012	0.00016	2.71

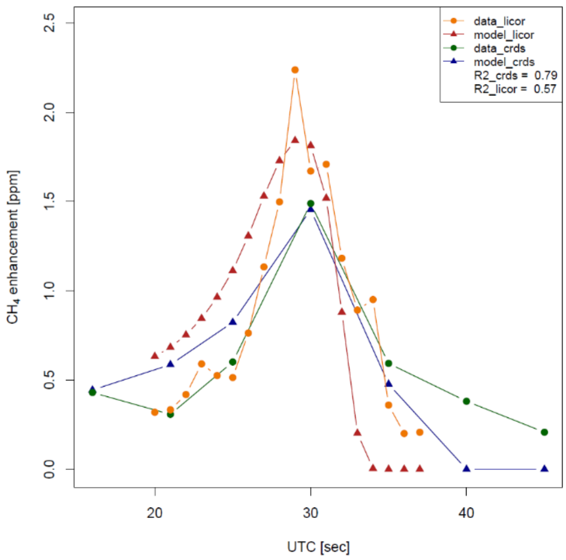

Figure S4. Example of a measured CH$_4$ excess* during plume crossing with OF-CEAS (yellow) and CRDS (green), as well as modelled gauss fits to data in red and blue, respectively. *This measurement was performed outside the release experiments and is shown here for illustrative purposes only, without going into the data in more detail.

Driving speed and choice of mobile vehicle

As measurement duration and therefore the measured peak area is directly related to the driving speed as the area increases with decreasing speed it is important to have a closer look on this for field measurements. Even if the methane enhancement is multiplied by the distance of the individual data points and thus the effect of the speed should not influence the data, a precise investigation during field measurements is an important verification. In order to test the influence of vehicle speed on the measurement results, two measurements with 10 transects each, were carried out during HD2 at a distance of 25 m at 20 km h^{-1} and 50 km h^{-1}. Lower driving speeds allow a better resolution of the peak with 8 data points at 20 km h^{-1} and only 5 data points at 50 km h^{-1} (see Fig. S5). The peak height is also affected and so the maximum CH_4 height for the peaks measured at 50 km h^{-1} is on average only 2/5 of the maximum peak height of the 20 km h^{-1} peaks. It should be noted, however, that this effect is particularly relevant for measurements taken close to the source, where plumes are narrower and more variable; at greater distances, where the plume shape tends to smooth out and become more Gaussian, the influence of driving speed on emission estimates may be less significant. Although no significant deviation of the estimated emission rate from the actual release rate can be observed in both scenarios we recommend that measurements are made at low driving speeds (≤ 30 km h^{-1}), especially close to the source.

The lightweight and compact OF-CEAS trace gas analyzer allows measurements to be taken by bicycle (Wietzel and Schmidt, 2023). The subject of the MA3 investigations was also the comparison between the choice of measurement vehicle (car or bicycle). Although the bicycle measurements are more variable (bike: std of 210 %; car: std of 120 %), both, the car and the bicycle measurements agree with the true release rate within their uncertainties (Fig. S6). Therefore, the bicycle set up is a good possibility to enable measurements on roads that are not accessible by car.

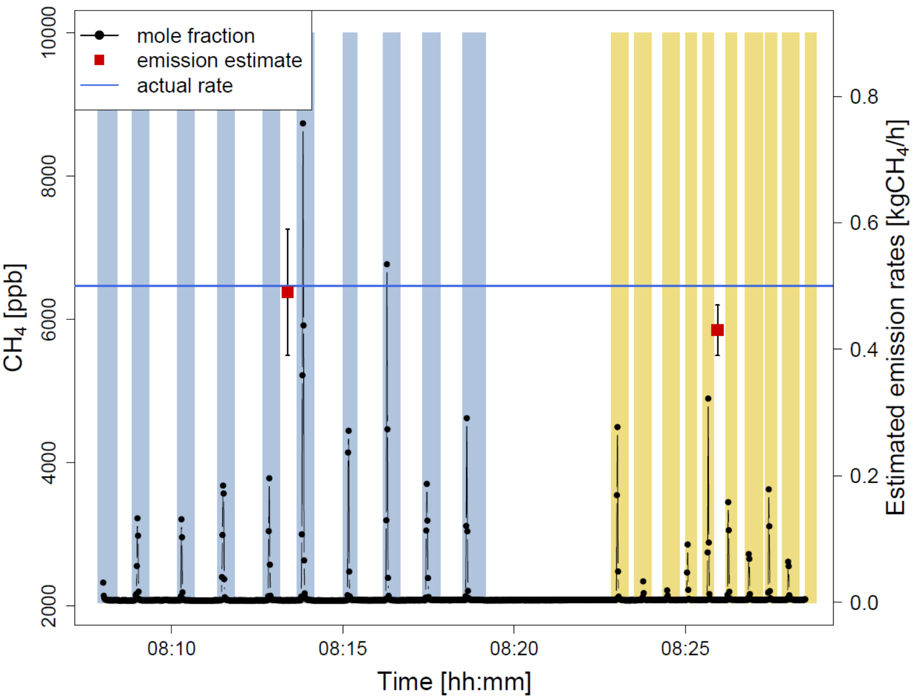

Figure S5. Time series with CH_4 mole fraction measured at different vehicle speeds highlighted (blue= 20 km h^{-1}; yellow= 50 km h^{-1}) with estimated release rates for the both driving speeds.

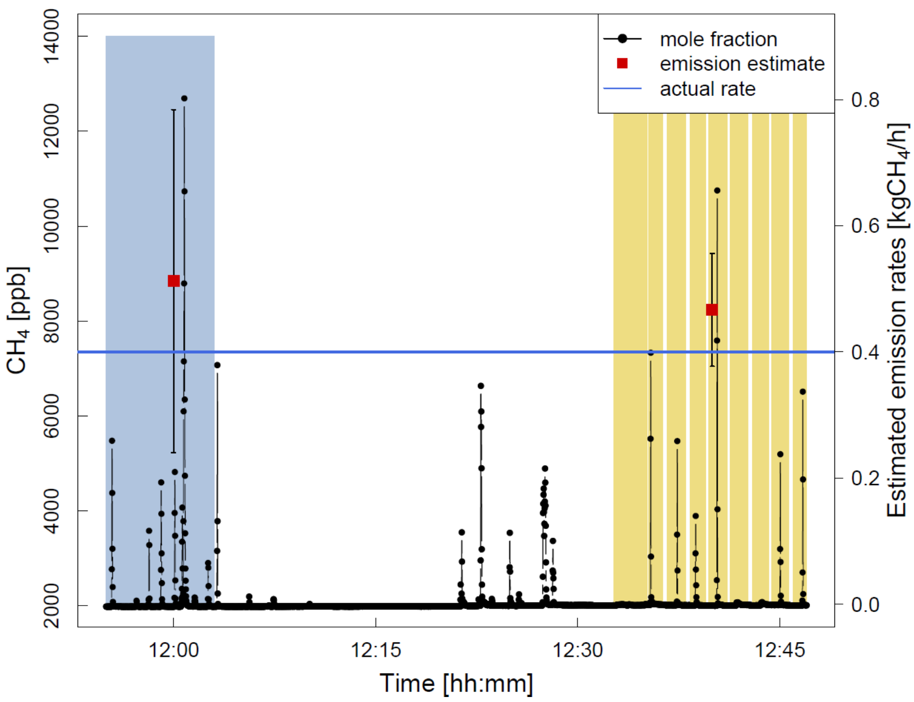

Figure S6. Time series with CH_4 mole fraction measured for 8 transects by bike (blue) and 11 transects by car (yellow) and determined emission rates in comparison to actual release rate for bike ad car, respectively.

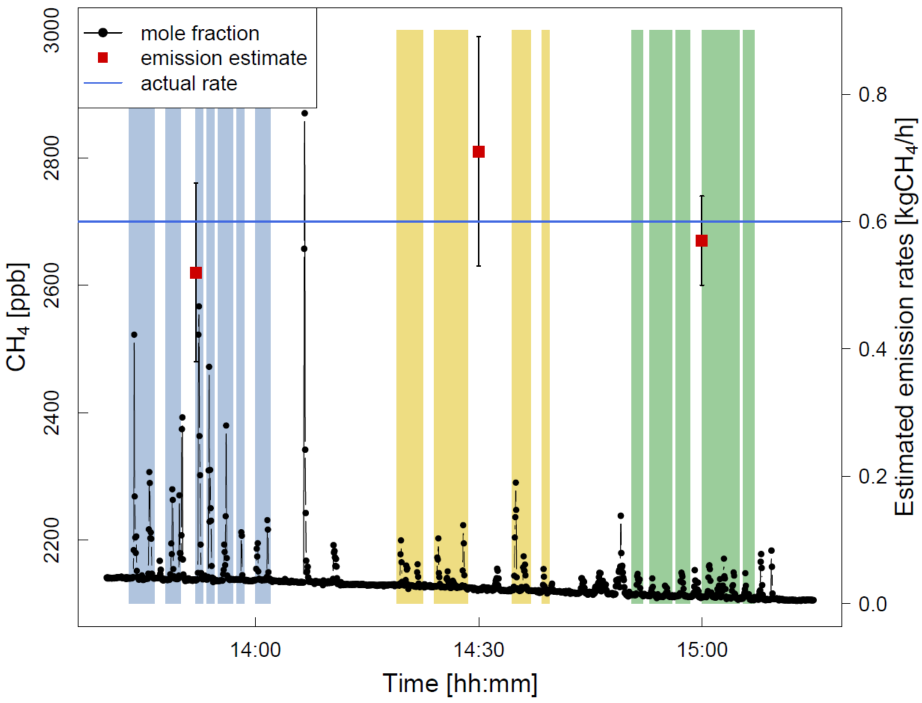

Figure S7. Time series with CH_4 mole fraction measured at different distances highlighted (blue =100 m, yellow = 250 m, green = 310 m) and determined emission rates in comparison to actual release rate for the three different distances.

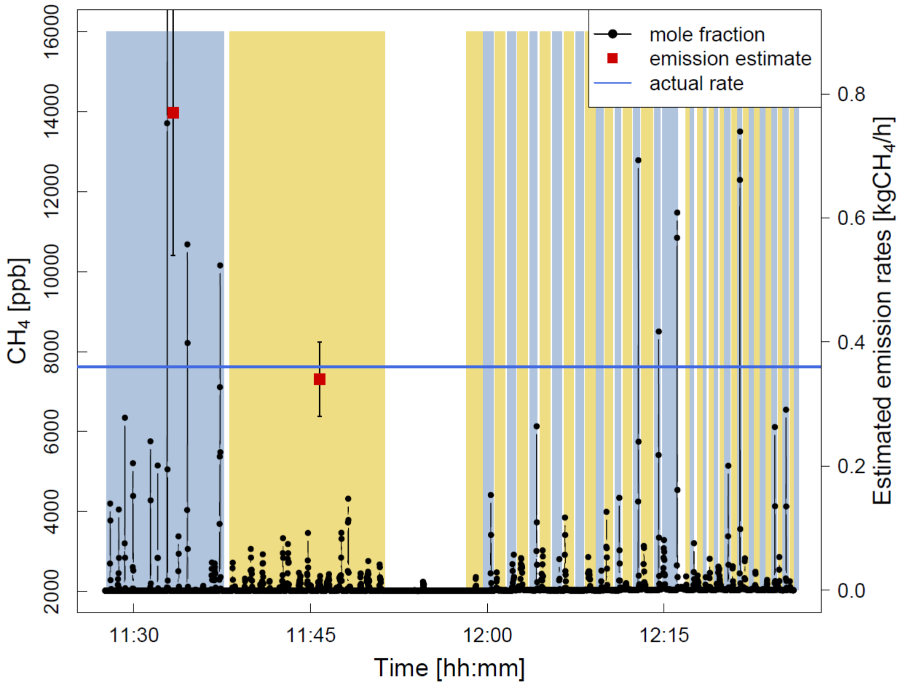

Figure S8. Controlled release experiment MA3 time series with CH_4 mole fraction measured at different distances highlighted (blue =14 m, yellow =36 m) and determined emission rates in comparison to actual release rate for the different distances.

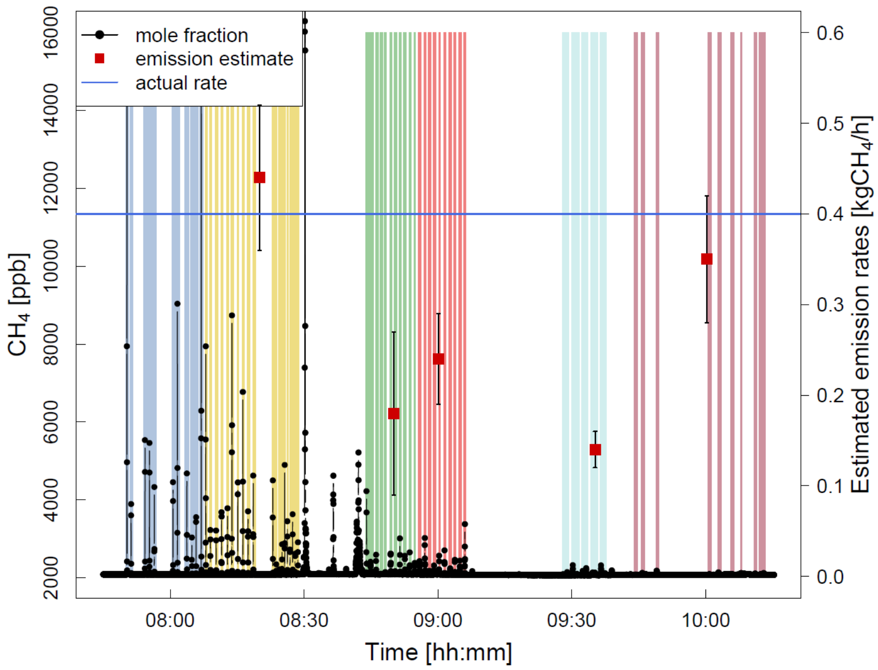

Figure S9. Controlled release experiment HD2 time series with CH_4 mole fraction measured at different distances highlighted blue (4 m), yellow (25 m), green (50 m), light red (70 m) light blue (120 m) and red (260 m) and determined emission rates in comparison to actual release rate for different distances. Note that the determined emission rate at the 4 m distance is with over 5700 $kgCH_4\ h^{-1}$ above the range of the second y-axis.

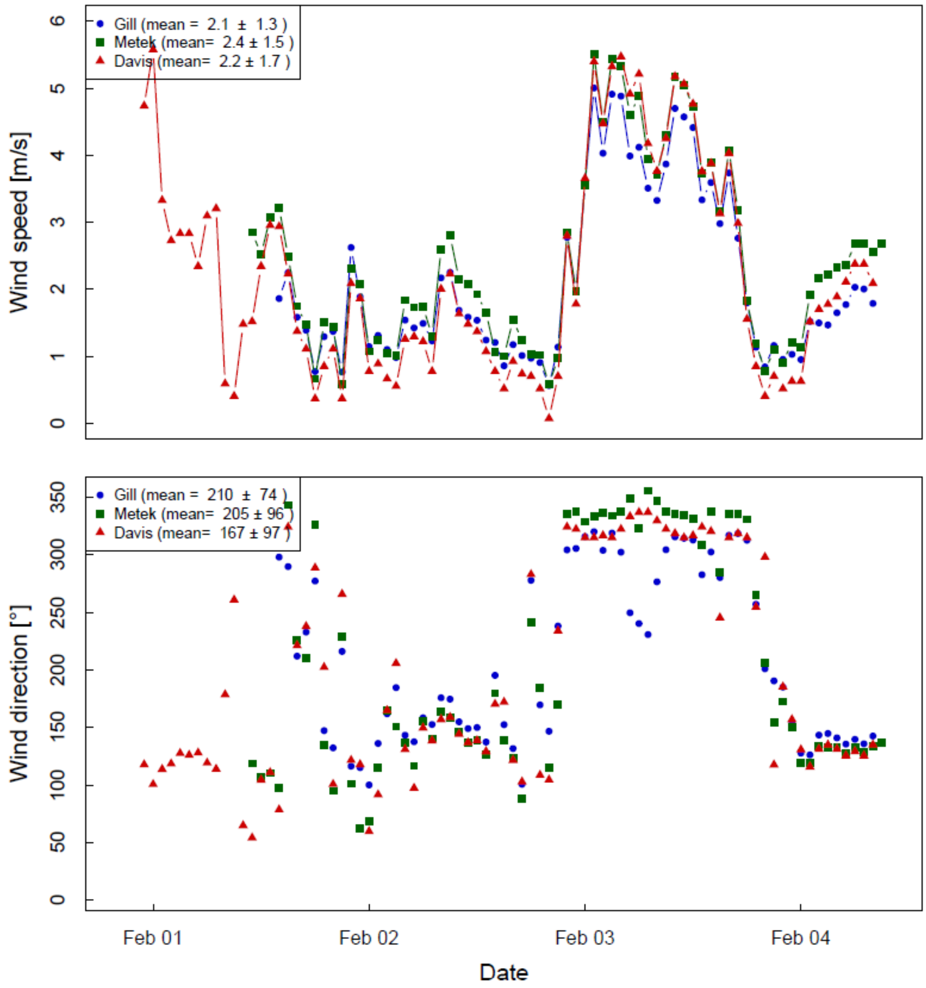

Figure S10. Wind speed (top) and wind direction (bottom) measured with the Gill (blue), Metek (green) and Davis (red) instruments installed stationary on the institute roof averaged hourly (February 2019).

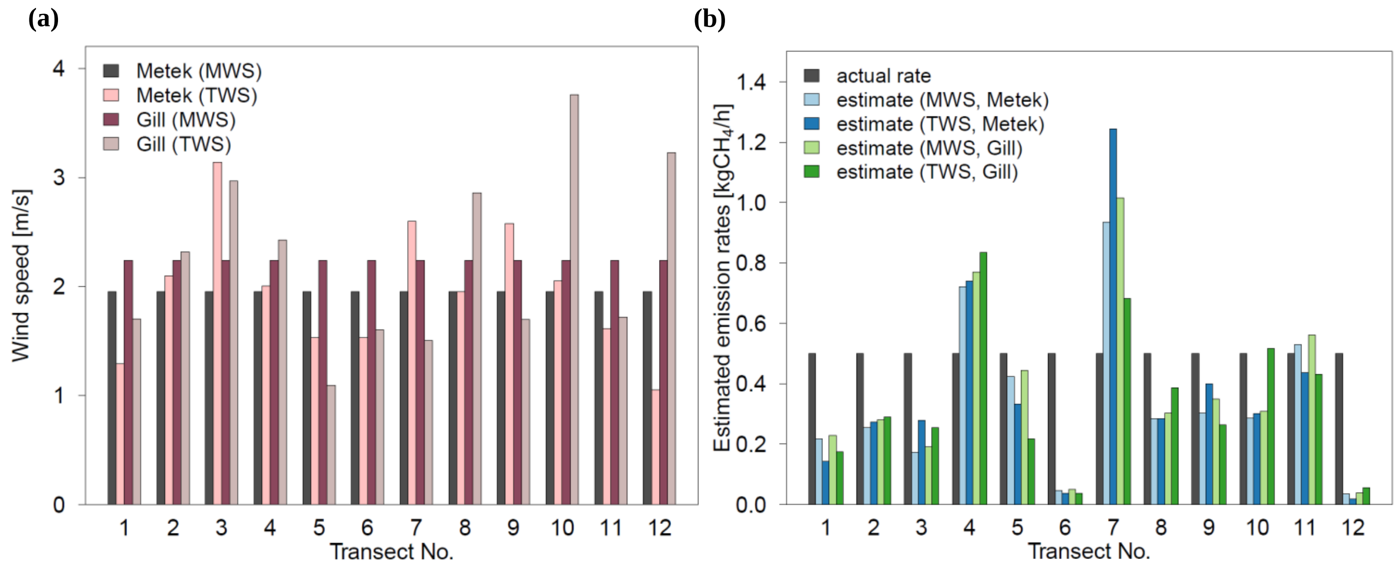

Figure S11. (a) Averaged wind speeds over each transect (TWS) or a set of transects (MWS) for the Metek and Gill instruments are shown for 10 transects performed during HD1. (b) Bar plot showing the emission rates calculated via mean wind speed (MWS) and transect wind speed (TWS) with wind measurements conducted using the Metek and Gill instruments, respectively, compared to the actual release rate.

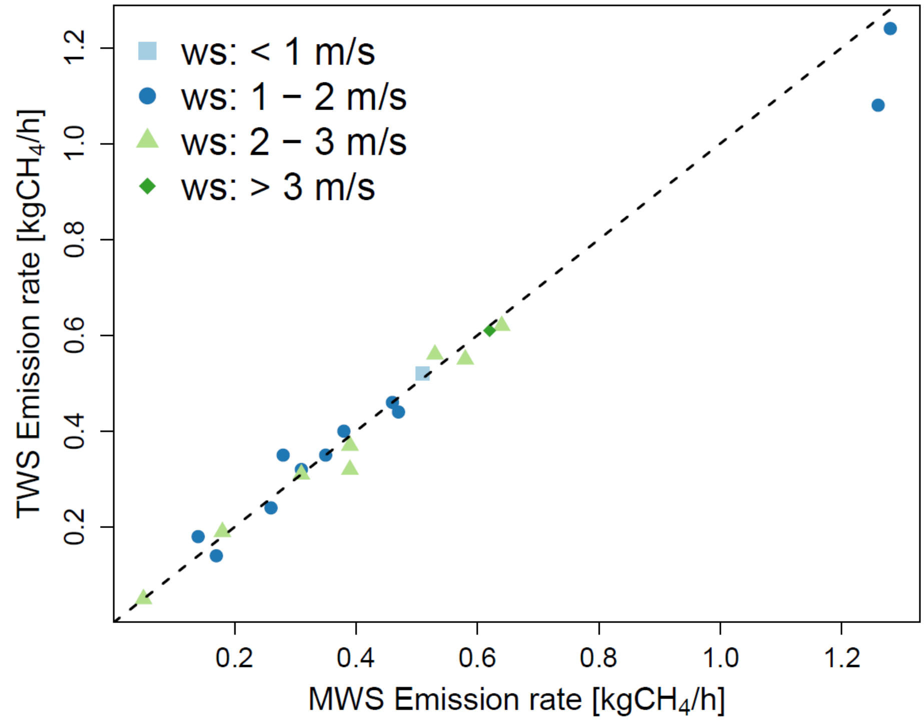

Figure S12. Comparison of CH_4 emission rates calculated using transect wind speed (TWS) versus those calculated using mean wind speed (MWS) for each controlled release during HD1–HD3. Data points are color-coded according to the measured wind speed during the releases. The dashed line represents the 1:1 reference line.

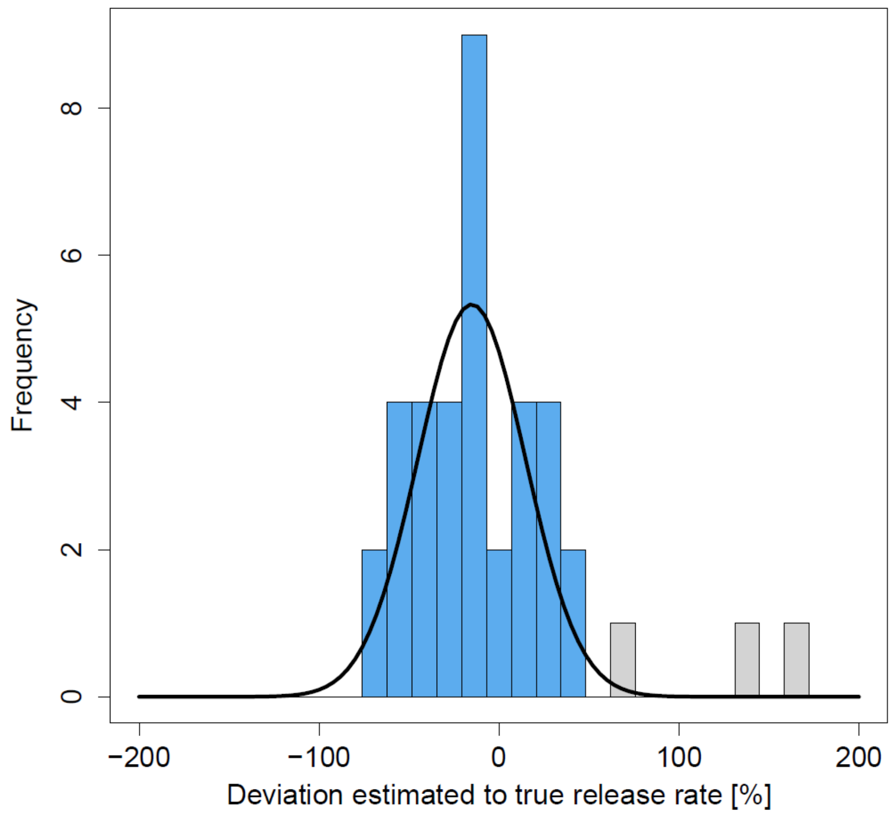

Figure S13. Histogram illustrating the distribution of mean estimated emission rates relative to the actual release rate across all six controlled release experiments conducted between 2018 and 2023. The black curve represents the normal distribution of the data, calculated using the mean and standard deviation. Grey data represent measurements at a distance of 14 m between air inlet and release source and are excluded from the normal distribution.

No.	Date	Emission rate [kg h^{-1}]	# Transects	# Peaks	Max CH_4 [ppm]	WD [°]	WS [ms^{-1}]	Solar radiation [W m^{-2}]	PGSC	Distance [m]
1	29.08.2016	3.74 ± 1.44	10	9	3.9	219	9.5	537	D	154
2	08.09.2016	5.90 ± 2.52	9	3	3.3	135	5.7	651	D	229
3	12.09.2016	0.58 ± 0.18	6	3	3.2	154	1.1	562	A-B	32
4	28.09.2016	7.85 ± 6.23	7	3	2.5	218	5.6	511	D	210
5	10.10.2016	3.46 ± 1.12	11	8	10.5	195	1.2	157	B	111
6	02.11.2016	9.29 ± 4.32	8	5	2.7	274	3.4	325	C	172
7	30.11.2016	4.97 ± 2.84	10	6	7.9	182	2.2	190	C	191
8	10.01.2018	13.64 ± 4.14	5	4	22.4	133	3.0	0	C	162
9	26.11.2018	4.46 ± 2.48	4	3	2.3	40	1.4	0	B	286
10	17.12.2018	6.34 ± 0.32	10	3	19.2	154	1.5	4	B	28
11	24.07.2019	5.65 ± 2.70	9	7	18.8	123	1.4	594	A-B	95
12	30.01.2020	10.15 ± 1.08	15	11	51.9	186	1.6	61	B	28
13	11.09.2020	10.94 ± 2.48	16	9	6.2	256	2.5	650	B-C	163
14	12.11.2020	5.94 ± 1.19	12	8	3.3	165	2.2	56	C	332
15	08.07.2022	4.54 ± 0.58	22	13	4.0	184	2.0	966	A-B	260
16	05.10.2022	3.10 ± 0.29	15	8	6.8	153	2.1	543	B	30
17	24.01.2023	6.77 ± 0.68	36	33	3.8	168	3.7	48	C	262
18	16.05.2023	5.76 ± 0.58	20	16	2.9	352	3.7	310	C	240
19	04.08.2023	5.69 ± 0.40	20	18	3.3	347	4.4	850	C-D	246
20	28.09.2023	4.79 ± 0.50	16	11	13.9	177	1.9	389	B	59
21	10.10.2023	4.54 ± 0.36	11	8	14.4	126	1.3	509	A-B	29
22	18.12.2023	6.08 ± 0.61	22	14	13.2	160	3.2	/	C	181
23	09.02.2024	5.00 ± 0.32	24	16	12.4	152	2.7	54	C	243
24	01.03.2024	6.12 ± 1.12	10	6	15.2	143	2.0	89	C	27
25	17.06.2024	4.97 ± 0.54	21	4	2.3	218	3.0	590	B-C	306
26	07.08.2024	2.88 ± 0.32	23	15	10.9	175	2.2	389	C	172

Table S4. Overview of measurements carried out between 2016 and 2024 at a local biogas plant. Determined CH_4 emission rates as well as measured meteorological parameter and several supplementing values are given for each measurement day.

Study	Country	Method	Plant type and number	Range of loss rate [%]	Average loss rate [%]
Bakkaloglu et al., 2021	UK	GPM	agricultural (6) waste (3)	0.02 - 8.1	3.7
Fredenslund et al., 2023	Denmark	Tracer release	agricultural (44)	0.3 - 40.6	4.7
Wechselberger et al., 2025	EU	Remote sensing, statistical	agricultural (49) waste (14)	0.3 – 6.5	2.8
This study	Germany	GPM	mixed waste and agricultural (1)	0.5 - 10.1	4.6

Table S5. Comparison of three studies on CH_4 loss rates at various biogas plants in Europe with this study.